Mapping the magneto-structural quantum phases of Mn_3O_4

M. Kim, X.M. Chen, E. Fradkin, P. Abbamonte, S.L. Cooper
Department of Physics and Frederick Seitz Materials Research Laboratory, University of Illinois, Urbana, Illinois 61801, USA
(Dated: February 25, 2010)

We present temperature-dependent x-ray diffraction and temperature- and field-dependent Raman scattering studies of single crystal Mn_3O_4, which reveal the novel magnetostructural phases that evolve in the spinels due to the interplay between strong spin-orbital coupling, geometric frustration, and applied magnetic field. We observe a structural transition from tetragonal to monoclinic structures at the commensurate magnetic transition at T_2=33K, show that the onset and nature of this structural transition can be controlled with an applied magnetic field, and find evidence for a field-tuned quantum phase transition to a tetragonal incommensurate or spin glass phase.

PACS numbers: 71.70.Ej, 73.43.Nq, 78.30.-j

Strong coupling among the spin, lattice, and orbital degrees of freedom in the geometrically frustrated spinel compounds [1] results in a rich variety of exotic magnetic and structural phases and properties that are of both scientific and technological interest. For example, the chromium-oxide spinels AB_2O_4 (A=Zn, Cd, Hg; B=Cr) exhibit three-dimensional spin-Peierls transitions involving coupled magnetic and structural transitions;[2-6] the vanadium-oxide spinels AB_2O_4 (A=Zn, Cd, Mn; B=V) display complex spin/orbital ordering and technologically useful phenomena such as large magnetoelastic and magnetodielectric effects;[7-14] and sulfer-based spinels such as FeB_2S_4 (B=Cr,Sc) [15] exhibit orbital-liquid or -glass ground states in which frustration prevents orbital ordering down to T=0. The rich magneto-structural phases of the spinels are thought to be governed by the interplay between spin-orbital coupling, applied magnetic field, and frustrated exchange interactions,[1,16] but there has been little experimental investigation of the microscopic details of this interplay.

The binary spinel Mn_3O_4 is a relatively simple system for experimentally studying the complex interplay between structure, spin-orbital coupling, and magnetic field in the spinels: in spite of its simpler chemical composition—with Mn ions at both tetrahedral (A=Mn^{2+}) and octahedral (B=Mn^{3+}) sites—Mn_3O_4 exhibits the rich magneto-structural transitions characteristic of more complex ternary magnetic spinels: Below T_C=43K, the spins in Mn_3O_4 exhibit Yafet-Kittel-type ferrimagnetic ordering, in which the net spin of the octahedrally coordinated Mn^{3+} spins is antiparallel to the [110] direction of the tetrahedrally coordinated Mn^{2+} spins, with pairs of Mn^{3+} spins canted by $\pm\theta_{YK}$ from the $[\bar{1}\bar{1}0]$ direction, where $\cos\theta_{YK}$=0.38 (0.33) at T=4.7K and $\cos\theta_{YK}$=0.40 (0.25) at T=29K for the "non-doubling" octahedral ("doubling" octahedral) site.[14,17] However, below T_1=39K, Mn_3O_4 develops an incommensurate sinusoidal or spiral spin structure of the Mn^{3+} spins; and below T_2=33K, Mn_3O_4 exhibits a commensurate spin structure in which the magnetic unit cell doubles the chemical unit cell.[17,18] Recent studies also show that the magnetic transitions in Mn_3O_4 are are associated with significant temperature- and field-dependent changes in the dielectric constant and lattice parameters, reflecting strong spin-lattice coupling in this material.[19,20]

In this paper, we report Raman spectroscopy and x-ray diffraction measurements of the temperature- and magnetic-field-dependent phases of single-crystal Mn_3O_4. These combined measurements offer a particularly clear, microscopic view of the diverse magneto-structural phases that can result from the interplay between strong spin-orbital coupling, geometric frustration, and applied magnetic field in the spinels; this includes evidence for a quantum phase transition to a tetragonal spin/orbital glass phase for intermediate fields with $H\|[1\bar{1}0]$, which we propose is caused by a field-tuned degeneracy between magneto-structural states.

A single-crystal sample of Mn_3O_4 was grown at the University of Illinois using a floating zone technique; the sample was identified as a single phase crystal using both x-ray powder diffraction with a Rigaku D-Max system and a pole figure analysis with a Phillips X'pert system. Field-dependent Raman measurements were performed as described previously [21] on an as-grown surface of single crystal Mn_3O_4 having a surface normal along the [110] direction. Temperature-dependent x-ray measurements were carried out using a Rigaku rotaflex RU-300 with a closed-cycle He refrigerator in the range of 10K to 75K. In addition, a Phillips MRD X'Pert was used for high precision measurements at room temperature. Both measurements were performed on the as-grown [110] surface of single crystal Mn_3O_4. A least squares program was used to determine the lattice parameters of the crystal from the data.

The room-temperature Raman spectrum of our Mn_3O_4 sample exhibits 5 phonon peaks, consistent with previous reports:[22] a T_{2g} symmetry mode at 290 cm^{-1}, an E_g symmetry mode at 320 cm^{-1}, T_{2g} symmetry modes at 375 cm^{-1} and 479 cm^{-1}, and an A_{1g} symmetry mode

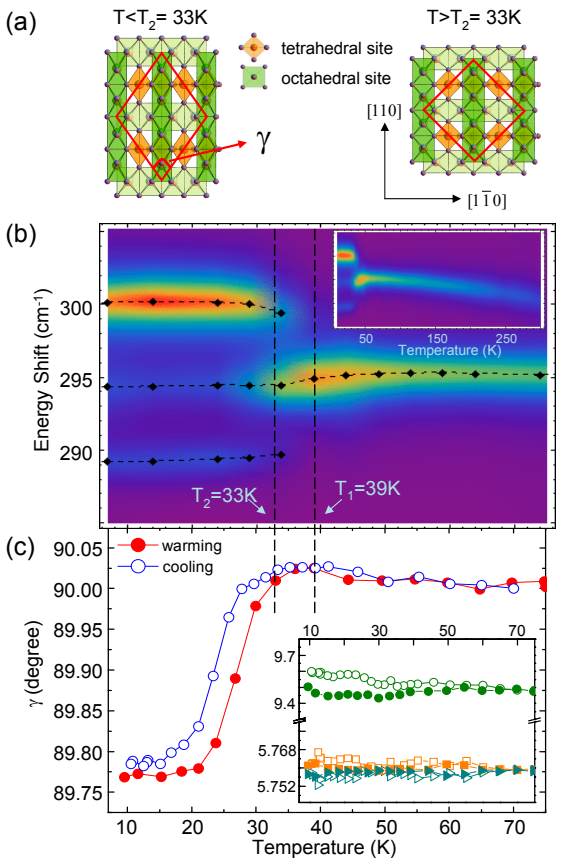

FIG. 1: (a) Illustrations of the monoclinic structure for T<T_2=33K and the tetragonal structure of Mn_3O_4 for T>T_2=33K. (b) Contour plot of the T_{2g} phonon mode intensity as functions of energy and increasing temperature, where red=700 counts and blue=0 counts. (inset) Contour plot of the T_{2g} phonon mode intensity over the full temperature range 7-290K. (c) Temperature dependence of γ—the angle between the a- and b-axis directions—as functions of increasing temperature (closed symbols) and decreasing temperature (open symbols). (inset) Temperature dependence [in K] of lattice constants a (squares), b (triangles), and c (circles) [in Å] for Mn_3O_4. Open (closed) symbols represent measurements taken with decreasing (increasing) temperature.

at 660 cm^{-1}.[22,23] In this paper, we focus on the lowest energy T_{2g} phonon mode, which is associated with Mn-O bond-stretching vibrations of the tetrahedral site ions.[22,23]

Fig. 1(b) shows the temperature dependence of the T_{2g} mode intensity and the T_{2g} mode energy and linewidth for light polarized along the [1$\bar{1}$0] crystallographic direction of Mn_3O_4. Three distinct temperature regimes can be identified: (i) T > T_1=39K – Above T_1=39K, the T_{2g} mode narrows and shifts to higher frequencies with decreasing temperature in a conventional manner, i.e., consistent with a temperature dependence governed by anharmonic (multi-phonon) effects.[24] (ii) T_2=33K < T ≤ T_1=39K – In the incommensurate magnetic phase regime between T_2=33 K and T_1=39K, the lowest T_{2g} mode decreases in energy slightly with decreasing temperature due to magnetoelastic effects, but exhibits no evidence for a change in structural symmetry. (iii) T < T_2=33K – Below the commensurate magnetic transition T_2=33K, the T_{2g} mode abruptly splits into three modes near 290 cm^{-1}, 295 cm^{-1}, and 300 cm^{-1}. This splitting is consistent with a tetragonal-to-monoclinic distortion below T_2, which splits the degenerate T_{2g} mode by expanding the Mn^{2+}-O^{2-} bond length along the easy-axis [110] direction and contracting the Mn^{2+}-O^{2-} bond length along the hard-axis [1$\bar{1}$0] direction (see illustrations, Fig. 1(a)). Note that the relative intensities of the three modes shown in Fig. 1(b) for T < T_2 confirm that the Mn^{2+}-O^{2-} bond length expands along the easy-axis [110] direction below T_2=33K: the higher-energy (∼300 cm^{-1}) split mode—which is associated with vibrations of the contracted Mn^{2+}-O^{2-} bond—exhibits the strongest light scattering intensity, indicating that the contracted Mn^{2+}-O^{2-} bond is oriented in the direction of the incident light polarization, i.e., along the [1$\bar{1}$0] direction. By contrast, the intensity of the lower-energy (∼290 cm^{-1}) split mode—which is associated with vibrations of the expanded Mn^{2+}-O^{2-} bond—has a substantially weaker intensity than the ∼300 cm^{-1} mode, consistent with an expansion of the Mn^{2+}-O^{2-} bond in a direction perpendicular to the incident light polarization, i.e., along the [110] direction.

To provide more definitive evidence for a tetragonal-to-monoclinic phase transition below T_2 in Mn_3O_4, temperature-dependent x-ray diffraction measurements were performed on the same crystal. Fig. 1(c) shows the temperature dependence of the lattice parameters a, b, c, and γ—the angle between a and b—as functions of both increasing ("warming") and decreasing ("cooling") temperature. While γ exhibits an abrupt decrease near T_2=33K—indicating an abrupt decrease in the angle between a- and b-axis directions at this temperature, the lattice parameters a and b exhibit no significant temperature dependence, and the lattice parameter c exhibits only a weak temperature dependence and hysteretic behavior. This behavior confirms that Mn_3O_4 exhibits a first-order tetragonal-to-monoclinic structural phase transition near T_2=33K, as illustrated schematically in Fig. 1(a). Notably, the observed monoclinic crystal structure we observe below T_2=33K is consistent with the spin structure that has been previously reported for Mn_3O_4 below T_2: the coplanar spin structure of the doubled unit cell has spins lying within the (1$\bar{1}$0) plane with a net spin along [110], in which the Mn^{3+} spins are canted by an angle $\pm\theta_{YK}$ from the [$\bar{1}\bar{1}$0] direction. This spin canting is associated with a tilting of the $d_{3z^2-r^2}$ orbitals of Mn^{3+} toward the [$\bar{1}\bar{1}$0] direction due to spin-orbital coupling, which results in a tilting of Mn^{3+} octahedra and an expansion of the Mn^{2+}-O^{2-} bond length along the [110] direction.[17,20] We also note that the tetragonal structure we observe for the incommensurate magnetic phase regime between T_2=33K and T_1=39K

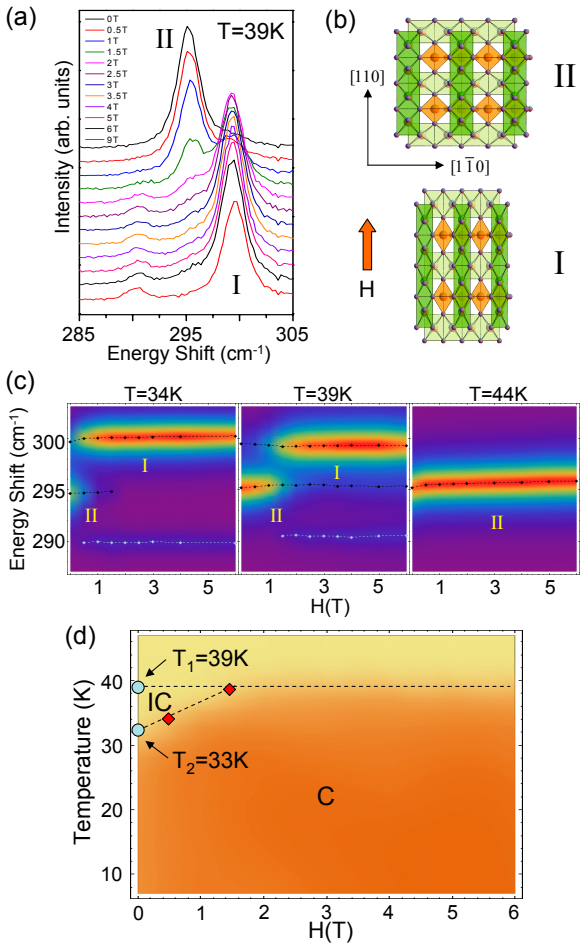

FIG. 2: (a) Field dependence of the Raman spectra at T=39K for H||[110]. (b) Illustrations of the Mn_3O_4 structure in (top) the low-field undistorted phase and (bottom) the high-field monoclinic phase. (c) Contour plots of the intensities of the split modes as functions of energy and field at (left) T=34K, (middle) 39K, and (right) 44K, where red=700 counts and blue=0 counts for H||[110]. (d) Phase diagram as functions of magnetic field (along [110]) and temperature; orange region=structure I, yellow region=structure II, IC=incommensurate magnetic phase, C=commensurate (cell-doubled) magnetic phase.

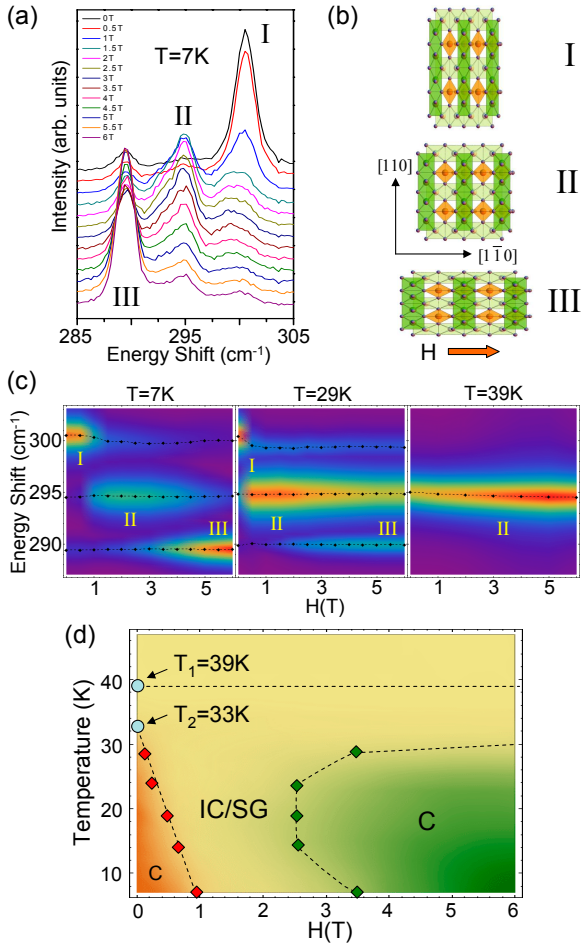

FIG. 3: (a) Field dependence of the Raman spectra at T=7K for a magnetic field applied along the hard-axis [1$\bar{1}$0] direction. (b) Illustrations of the Mn_3O_4 structure in (top) the low-field monoclinic phase, (middle) the intermediate undistorted tetragonal phase, and (bottom) the high-field monoclinic phase. (c) Contour plots of the intensities of the split modes as functions of energy and field at (left) T=7K, (middle) 29K, and (right) 39K, where red=700 counts and blue=0 counts for H||[1$\bar{1}$0]. (d) Phase diagram as functions of magnetic field (along [1$\bar{1}$0]) and temperature; orange region=structure I, yellow region=structure II, green region=structure III, IC/SG=incommensurate or spin glass magnetic phase, and C=commensurate (cell-doubled) magnetic phase.

(Fig. 1(b)) is consistent with the presence of an axially symmetric spiral spin structure [17] in this temperature regime.

The distinctive Raman spectroscopic signatures associated with the different magneto-structural phases in Mn_3O_4—illustrated in Fig. 1(b)—offer a convenient method for investigating the phases induced with an applied magnetic field. Fig. 2 illustrates the field-induced structural phases of Mn_3O_4 for fields applied along the easy-axis [110] direction. Fig. 2(a) and the left and middle plots of Fig. 2(c) show that, in the incommensurate magnetic phase regime T_2=33K < T ≤ T_1=39K, the ∼295cm^{-1} mode associated with the undistorted tetragonal phase (structure II in Fig. 2(b)) exhibits a field-induced splitting similar to that induced upon cooling below T_2=33K in zero magnetic field (Fig. 1(b)). Thus, in the incommensurate magnetic phase, an applied magnetic field along the easy axis [110] direction induces a tetragonal-to-monoclinic distortion in Mn_3O_4 by forcing the Mn^{3+} spins to order within the (1$\bar{1}$0) plane and inducing the cell-doubled coplanar magnetic structure associated with the monoclinic structure (see Fig. 2(b)). This strong magnetoelastic response at rather modest fields likely arises from a field-induced increase—via spin-orbit coupling—in the hybridization between the $d_{3z^2-r^2}$ and d_{xy} orbitals of Mn^{3+} for H||[110], and demonstrates that the magnetostructural states I and II in Fig. 2(b) have

very similar free energies. Fig. 2(d) summarizes the different magnetic/structural phases of Mn_3O_4 as functions of magnetic field and temperature for H‖[110].

A richer magneto-structural phase diagram is observed when the magnetic field is applied along the hard-axis [1$\bar{1}$0] direction of Mn_3O_4, as illustrated in Fig. 3. Figs. 3(a) and 3(c) show that three different phase regimes are apparent for H‖[1$\bar{1}$0] at T=7 K. For H < 1 T, the high-energy 300cm^{-1} mode is the dominant mode, indicating that the monoclinic distortion with an expanded Mn^{2+}-O^{2-} bond length along the easy-axis [110] direction (structure I) persists at low fields. On the other hand, at high magnetic fields, i.e., for H > 4T for T=7K, Figs. 3(a) and (c) show that the low-energy 290cm^{-1} mode is most intense, indicating a monoclinic phase in which the field reorients the Mn spin—and expands the Mn^{2+}-O^{2-} bond lengths—along the hard-axis [1$\bar{1}$0] direction (structure III).

Most remarkably, however, Figs. 3(a) and 3(c) show that the field-induced transition from a monoclinic distortion with M‖[110] to a monoclinic distortion with M‖[1$\bar{1}$0] is not abrupt, but occurs via an intermediate field regime (1T < H < 4T) in which the dominant mode is the ∼295cm^{-1} mode, i.e., the mode associated with the undistorted tetragonal phase (structure II in Figs. 3(b) and 3(c)) observed in the paramagnetic and incommensurate phases above T_2=33K for H=0 (Fig. 1(b)). We suggest that the quantum phase transition to this intermediate phase is a transition from a ferrimagnetic, monoclinic phase with M‖[110], to a "spin/orbital" glass phase—in which the Mn spins are randomly oriented along the [110] and [1$\bar{1}$0] directions—or to an incommensurate spiral spin phase; both of these possibilities are consistent with a tetragonal structure (see Fig. 1(b)). Fig. 3(c) shows that, with increasing temperatures, this field-induced tetragonal regime becomes more pronounced. Fig. 3(d) summarizes the different magnetic/structural phases of Mn_3O_4 as functions of magnetic field and temperature for H‖[1$\bar{1}$0].

The results summarized in Fig. 3(d) indicate that the competition between spin-orbital coupling, geometrical frustration, and applied magnetic field in Mn_3O_4 leads to an incommensurate—or even glassy—spin state at T=0 that is sandwiched—as a function of applied field with H‖[1$\bar{1}$0]—between commensurate spin phases. The observation of a quantum phase transition to an intermediate incommensurate or spin-glass tetragonal phase (structure II in Fig. 3(b))—rather than a simple metamagnetic transition between or coexistence of commensurate ferrimagnetic phases (structures I and III in Fig. 3(b)) at intermediate fields—likely reflects the importance of spin-lattice coupling in Mn_3O_4, wherein the balancing of elastic and magnetic energies favors the formation of a more isotropic magnetostructural configuration at intermediate fields with H‖[1$\bar{1}$0]. Indeed, this more isotropic magnetostructural configuration (II) appears to be the means by which Mn_3O_4 resolves the frustration that arises from the field-induced degeneracy between M‖[110] and M‖[1$\bar{1}$0] spin configurations at intermediate field values with H‖[1$\bar{1}$0]. Field-dependent neutron scattering and heat capacity measurements would be useful for clarifying the nature of the spin configuration and entropy of this highly frustrated field-induced state. It is also important to study the T∼0 spin dynamics of this intermediate-field isotropic phase, in particular to explore the extent to which quantum critical fluctuations govern the dynamics in this frustrated phase regime.

In summary, combined temperature- and field-dependent Raman scattering and temperature-dependent x-ray scattering studies provide a clear microscopic view of the diverse and complex magnetostructural phases that evolve in the spinel material Mn_3O_4 due to the interplay between spin-orbital coupling, geometrical frustration, and applied magnetic field. In addition to identifying the specific structural phases associated with the different magnetic states observed in Mn_3O_4 with H=0, we have identified the microscopic magnetostructural changes that are associated with the novel magnetodielectric behavior previously observed for this material. Most interesting is the observation of a quantum phase transition to a structurally isotropic, incommensurate/disordered spin state for intermediate fields with H‖[1$\bar{1}$0], which reflects a compromise this system takes to accommodate the frustration imposed by a field-induced degeneracy between differing magnetostructural states.

This material is based on work supported by the U.S. Department of Energy, Division of Materials Sciences, under Award No. DE-FG02-07ER46453, through the Frederick Seitz Materials Research Laboratory at the University of Illinois at Urbana-Champaign, and by the National Science Foundation under Grant NSF DMR 08-56321.

[1] P. W. Anderson, Phys. Rev. **102**, 1008 (1956).
[2] S.-H. Lee, C. Broholm, T. H. Kim, W. Ratcliff, II, and S-W. Cheong, Phys. Rev. Lett. **84**, 3718 (2000).
[3] A. B. Sushkov, O. Tchernyshyov, W. Ratcliff, S. W. Cheong, and H. D. Drew, Phys. Rev. Lett. **94**, 137202 (2005).
[4] J.-H. Chung *et al.*, Phys. Rev. Lett. **95**, 247204 (2005).
[5] R. Valdes Aguilar, A. B. Sushkov, Y. J. Choi, S.-W. Cheong, and H. D. Drew, Phys. Rev. B **77**, 092412 (2008).
[6] M. Matsuda *et al.*, Nat. Phys. **3**, 397 (2007).
[7] M. Onoda and J. Hasegawa, J. Phys.: Condens. Matter **15**, L95 (2003).
[8] H. Tsunetsugu and Y. Motome, Phys. Rev. B **68**, 060405(R) (2003).
[9] S.-H. Lee *et al.*, Phys. Rev. Lett. **93**, 156407 (2004).
[10] Z. Zhang *et al.*, Phys. Rev. B **74**, 014108 (2006).
[11] T. Suzuki, M. Katsumura, K. Taniguchi, T. Arima, and T. Katsufuji, Phys. Rev. Lett. **98**, 127203 (2007).
[12] H. Takei, T. Suzuki, and T. Katsufuji, Appl. Phys. Lett. **91**, 072506 (2007).

[13] T. Suzuki, K. Adachi, and T. Katsufuji, J. Phys.: Conf. Ser. **31**, 235 (2006).
[14] J.-H. Chung *et al.*, Phys. Rev. B **77**, 054412 (2008).
[15] V. Tsurkan *et al.*, J. Phys. Chem. Solids **66**, 2036 (2005); N. Büttgen *et al.*, New Journal of Physics **6**, 191 (2004).
[16] S. B Lee and L. Balents, Phys. Rev. B **78**, 144417 (2008).
[17] G. B. Jensen and O. V. Nielsen, J. Phys. C **7**, 409 (1974).
[18] B. Chardon and F. Vigneron, J. Magn. Magn. Mater. **58**, 128 (1986).
[19] R. Tackett *et al.*, Phys. Rev. B **76**, 024409 (2007).
[20] T. Suzuki and T. Katsufuji, Phys. Rev. B **77**, 220402(R) (2008).
[21] J. F. Karpus, R. Gupta, H. Barath, S. L. Cooper, and G. Cao, Phys. Rev. Lett. **93**, 167205 (2004).
[22] C. M. Julien and M. Massot, J. Phys.: Condens. Matter **15**, 3151 (2003); B. Ammundsen *et al.*, J. Phys. Chem. B **103**, 5175 (1999); L. Malavasi *et al.*, Phys. Chem. Chem. Phys. **4**, 3876 (2002).
[23] Following reference 22, we use the cubic space group notation to index the Raman-active phonons in tetragonal Mn_3O_4 because the Raman spectrum of Mn_3O_4 corresponds well to those of cubic spinels.
[24] D. Mihailovic, K. F. McCarty, and D. S. Ginley, Phys. Rev. B **47**, 8910 (1993).